Click Here for Full Article

Comparison of carbon monoxide measurements by TES and MOPITT: Influence of a priori data and instrument characteristics on nadir atmospheric species retrievals

M. Luo,[1] C. P. Rinsland,[2] C. D. Rodgers,[3] J. A. Logan,[4] H. Worden,[1] S. Kulawik,[1] A. Eldering,[1] A. Goldman,[5] M. W. Shephard,[6] M. Gunson,[1] and M. Lampel[7]

[1]   Comparisons of tropospheric carbon monoxide (CO) volume mixing ratio profiles and total columns are presented from nadir-viewing measurements made by the Tropospheric Emission Spectrometer (TES) on the NASA Aura satellite and by the Measurements of Pollution in the Troposphere (MOPITT) instrument on the NASA Terra satellite. In this paper, we first explore the factors that relate the retrieved and the true species profiles. We demonstrate that at a given location and time the retrieved species profiles reported by different satellite instrument teams can be very different from each other. We demonstrate the influence of the a priori data and instrument characteristics on the CO products from TES and MOPITT and on their comparisons. Direct comparison of TES and MOPITT retrieved CO profiles and columns show significant differences in the lower and upper troposphere. To perform a more proper and rigorous comparison between the two instrument observations we allow for different a priori profiles and averaging kernels. We compare (1) TES retrieved CO profiles adjusted to the MOPITT a priori with the MOPITT retrievals and (2) the above adjusted TES CO profiles with the MOPITT profiles vertically smoothed by the TES averaging kernels. These two steps greatly improve the agreement between the CO profiles and the columns from the two instruments. No systematic differences are found as a function of latitude in the final comparisons. These results show that knowledge of the a priori profiles, the averaging kernels, and the error covariance matrices in the standard data products provided by the instrument teams and understanding their roles in the retrieval products are essential in quantitatively interpreting both retrieved profiles and the derived total or partial columns for scientific applications.

1.   Introduction

[2]   Measurements of radiance spectra at the top of atmosphere from spaceborne instruments have been used to derive profiles or total columns of the atmospheric constituents such as CO with nearly continuous global coverage. Several currently operating remote sensing instruments are measuring CO distributions in the troposphere, including Measurements of Pollution in the Troposphere (MOPITT) [*Drummond and Mand*, 1996; *Deeter et al.*, 2003; *Edwards et al.*, 2004; *Clerbaux et al.*, 2004] and the Tropospheric Emission Spectrometer (TES) [*Beer et al.*, 2001; *Beer*, 2006; *Rinsland et al.*, 2006]. All remote sensing instruments have limitations in terms of their vertical, spatial and temporal resolution. One of the main difficulties in interpreting the species profiles or their corresponding columns from satellite measurements is to understand the influence of the a priori assumptions and the instrument characteristics on the final retrieved products provided by the instrument science teams. Treating these products as true local values for the given species in the atmosphere may result in misleading conclusions. This consideration is important in all applications of the satellite data, including validation, assimilation into models, inversion studies to test emission inventories, and model evaluation.

[3]   Carbon monoxide in the troposphere is routinely retrieved from thermal infrared measurements by TES and

---

[1]Jet Propulsion Laboratory, California Institute of Technology, Pasadena, California, USA.
[2]NASA Langley Research Center, Hampton, Virginia, USA.
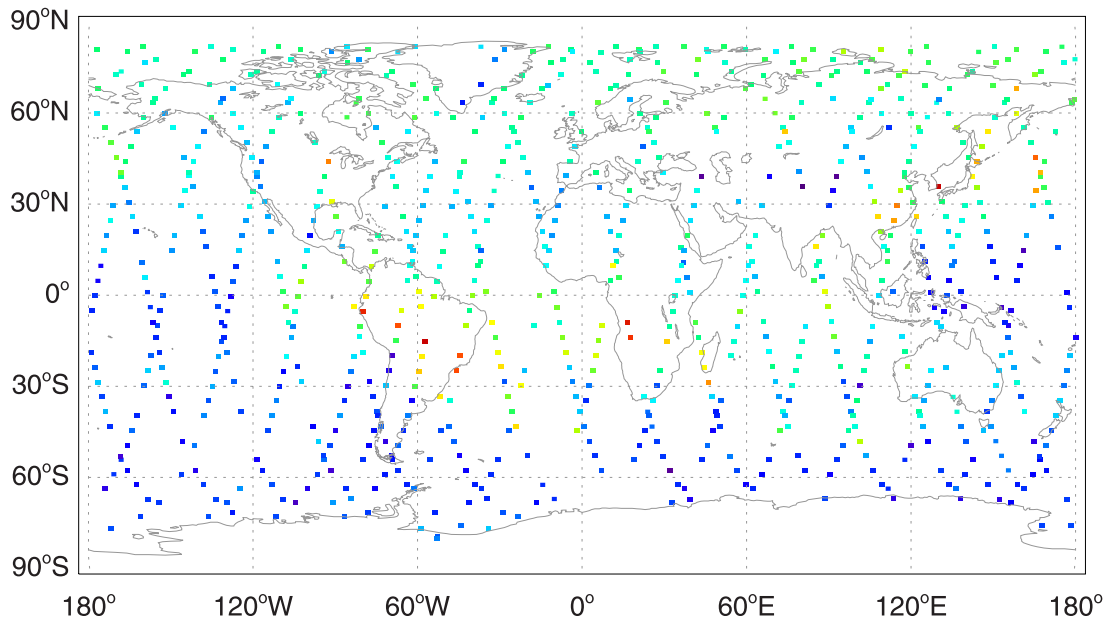[3]Clarendon Laboratory, Oxford University, Oxford, UK.
[4]Division of Engineering and Applied Sciences, Harvard University, Cambridge, Massachusetts, USA.
[5]Department of Physics, University of Denver, Denver, Colorado, USA.
[6]Atmospheric and Environmental Research Incorporated (AER), Lexington, Massachusetts, USA.
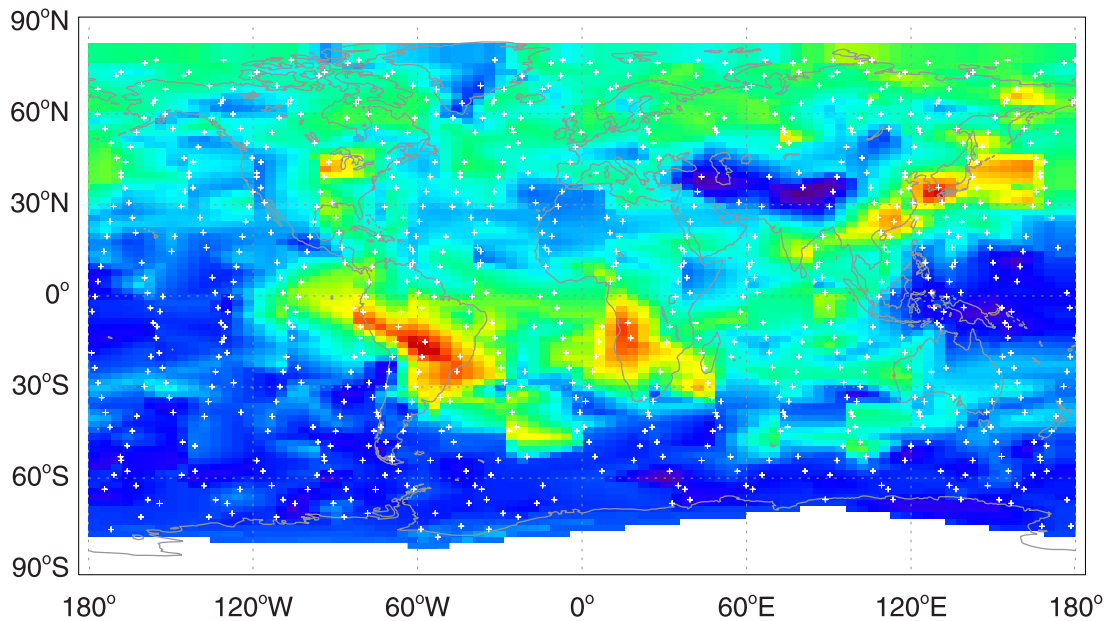[7]Raytheon Information Solutions, Pasadena, California, USA.

Figure 1. Tropospheric Emission Spectrometer (TES) CO total column (molecules/cm^2) calculated from profile retrieval for measurements in a global survey period of 20–21 September 2004 (data version 002). (top) TES CO columns at observation geolocations with enlarged symbols. The actual footprint size for a nadir observation is approximately 5 × 8 km. (bottom) the TES CO column interpolated globally with the measurement geolocations marked in white crosses. The enhanced CO seen in South America and Africa is due to biomass burning, and in other places in the Northern Hemisphere it is due to pollution.
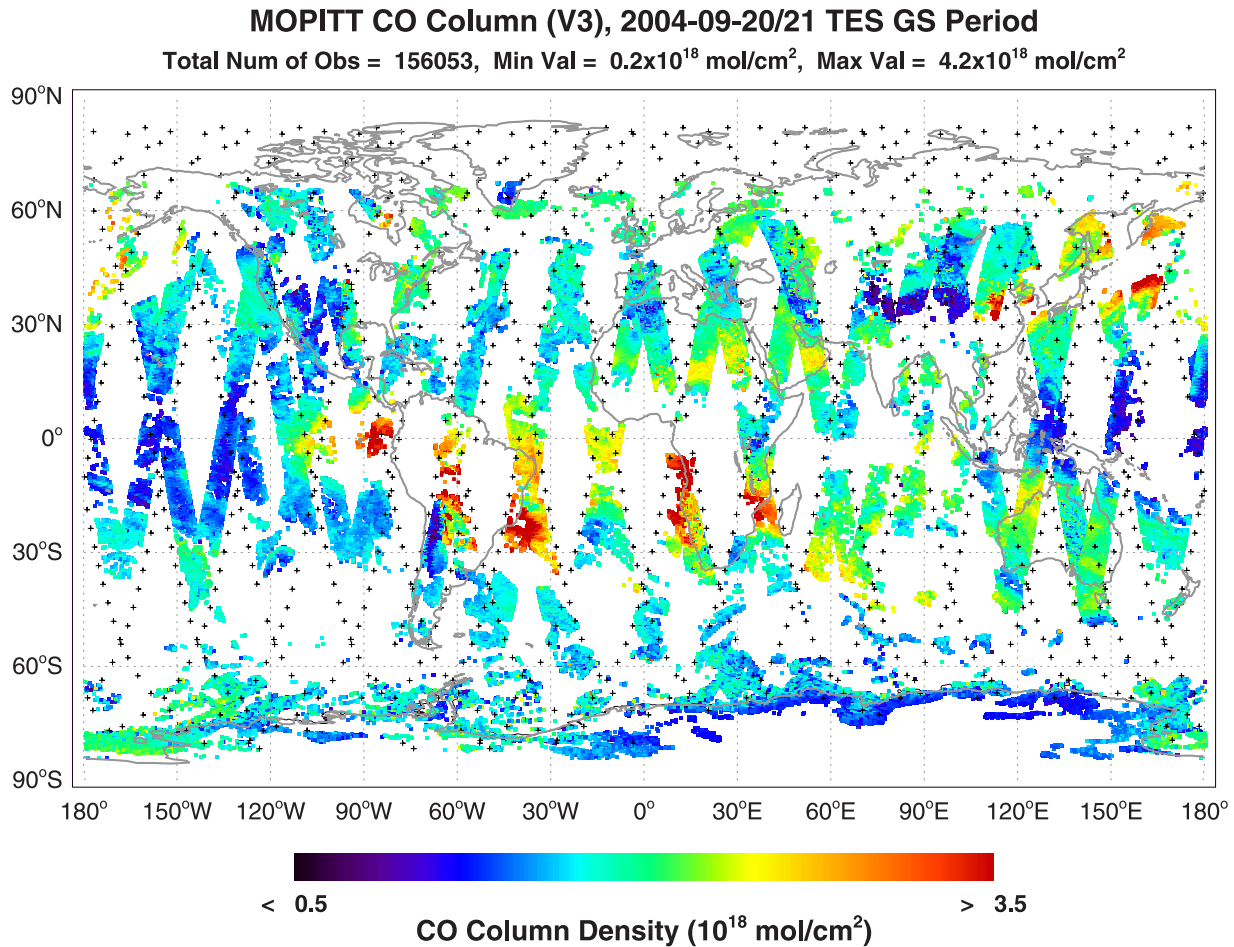
MOPITT CO Column (V3), 2004-09-20/21 TES GS Period

Total Num of Obs = 156053, Min Val = 0.2×10^{18} mol/cm^2, Max Val = 4.2×10^{18} mol/cm^2

CO Column Density (10^{18} mol/cm^2)

Figure 2. CO total columns from Measurements of Pollution in the Troposphere (MOPITT) measurements during the period of a TES global survey of 20–21 September 2004 (data version 3). Similar to the global CO columns of TES in Figure 1, the MOPITT CO field shows enhanced CO in regions of biomass burning and high-pollution sources. Overlaid black cross symbols are the TES geolocations.

MOPITT instruments, on board Aura and Terra satellites launched in July 2004 and December 1999, respectively. The MOPITT CO products have been validated by comparing to aircraft and ground-based measurements [*Emmons et al.*, 2004]. Similar validation is being carried out for TES data [*Osterman et al.*, 2005]. Comparisons between global data sets from TES and MOPITT are used to provide initial confidence in TES CO retrievals. Figure 1 shows TES CO columns from one global survey (~26 hrs) on 20–21 September 2004, plotted at observation geolocations and interpolated to form a global image. Figure 2 shows MOPITT CO column data for the same time period. The CO global distributions provided by the two instruments agree well qualitatively. For example, the enhanced CO sources in South America and South Africa due to biomass burning and in polluted regions of East Asia are seen by both instruments.

[4] Quantitative comparisons between global CO fields given by TES and MOPITT data products are presented. Differences are expected, because of the influence of different a priori data and of the instrument characteristics to the retrieved products. In this paper we follow the procedure suggested by *Rodgers and Connor* [2003] for proper comparisons of species profiles and columns derived from different observing systems and illustrate comparisons of CO profiles adjusted for different a priori assumptions and averaging kernels.

2. Retrievals of the CO Profiles From Nadir Remote Sensing Measurements

[5] Nadir spaceborne remote sensing instruments make spectral radiances measurements that are mainly due to attenuated surface emission at the top of the atmosphere. An optimal estimation method is commonly used to derive profiles of the atmospheric species from the measurement with the use of a priori data to constrain the retrieval results [*Rodgers*, 2000]. Some constraints, either explicitly or implicitly applied, are necessary for retrievals to have a unique solution so that the agreement between radiance measurement and the atmospheric radiation model calculations with the species profiles is consistent within the measurement noise, and so that the retrieved profiles are associated with errors that improve on the uncertainties prior to the measurements.
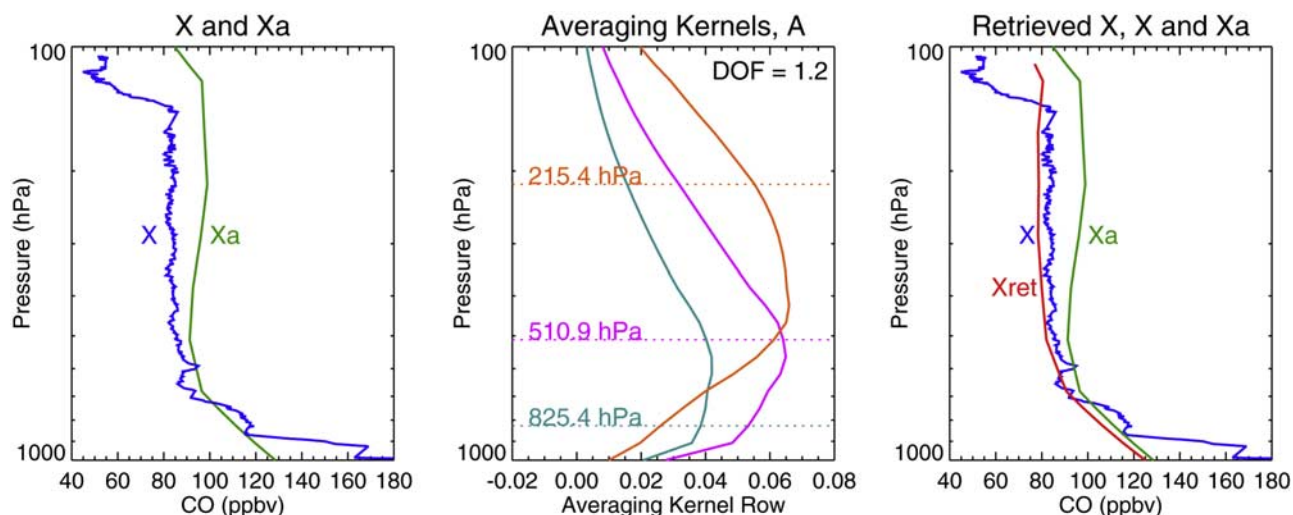
Figure 3. A simulation illustrating the relationship among true, a priori, and the retrieved CO profiles. (left) True CO profile (blue) obtained from in situ measurements of CO from the Argus instrument during Aura Validation Experiment near Houston, 31 October 2004, and the a priori profile (green) used by TES in the closest location. (middle) TES averaging kernel rows corresponding to 825, 510, and 215 hPa for the retrieved profile at the location. The DOF for the TES retrieval is 1.2. (right) Calculated retrieved profile for CO (x_{ret}, red) together with the true (x) and the a priori (x_a). The number of CO retrieval levels used in the simulation is 25 between 1000 and 100 hPa.

[6] The optimal retrieval method used by both TES and MOPITT in retrieving tropospheric CO profiles follows that of *Rodgers* [2000]. The retrieved profile (x_{ret}) may be expressed as the linear combination of the weighted true profile (x) and the a priori profile (x_a),

$$x_{ret} = Ax + (I - A)x_a + \varepsilon \qquad (1)$$

where A is the averaging kernel matrix and ε is the retrieval error due to random errors in the measurement and systematic errors in the forward model, e.g., the error in the atmospheric temperature retrieval.

[7] Equation (1) establishes the relationship between the retrieved and true species profiles and is crucial in understanding retrieval data (x_{ret}) for all data applications. With an ideal averaging kernel of unity, $A = I$, the retrieval x_{ret} would equal the true profile x plus the noise. However the current remote sensing systems, e.g., TES or MOPITT, have averaging kernels with values far from unity across the whole measurement domain. The retrieved profile is the combination of the unknown true profile (x) vertically smoothed by rows of the averaging kernel matrix (1st term) and the a priori profile weighted by ($I - A$) (2nd term). The averaging kernels (the rows of the averaging kernel matrix, A) are the key in this relationship. The averaging kernels are determined by the sensitivities of the spectral measurements to the species concentrations at different atmospheric altitudes, the signal-to-noise ratios of the measurements, and the a priori constraints used in retrievals.

[8] Quantitative comparison of profiles derived from radiances measured by two different instruments requires knowledge of how each algorithm applies constraints, how the vertical structure of the atmosphere is approximated, how profiles of temperature and molecular interferences are retrieved, and how clouds are detected and modeled.

[9] Figures 3 and 4 are two examples illustrating the relationship between the retrieved profile (x_{ret}), the assumed true profile (x) and the a priori profile (x_a) in equation (1), for two atmospheric conditions. The assumed true profiles are taken from the in situ CO measurements via the Argus (http://cloud1.arc.nasa.gov/crystalface/WB57_files/argus2.pdf) and DACOM (Differential Absorption CO Measurement) [*Sachse et al.*, 1987] instruments onboard WB-57 and DC-8 aircrafts during the Aura Validation Experiment near Houston in October 2004 (http://cloud1.arc.nasa.gov/ave-houston/index.cgi) and Portsmouth NH in February 2005 (http://www.espo.nasa.gov/ave-polar/index.html), respectively. These in situ profiles are extended beyond the minimum in situ measurement pressure by shifted a priori profiles before applying A in equation (1). The a priori profiles and the averaging kernels for CO used in equation (1) are those from the TES instrument at the times and locations closest to the aircraft measurements. TES reports about 25 levels for the profile and the corresponding averaging kernels in the troposphere. There are distinct differences in the averaging kernels from TES for the two cases. For example, the peaks of A in Figure 3 for 215 and 825 hPa are somewhat higher and lower in altitude than that of 511 hPa, while the peaks of A in Figure 4 for all three pressures are near 500–600 hPa. The main reason for the difference is the temperature at the Earth surface: the warmer surface in October near Houston (Figure 3) resulted in larger signal-to-noise ratios in the spectral measurements. The retrievals near Houston therefore contain more information on the CO profile shape than those near Portsmouth. The peak pressures of the averaging kernels indicate that the retrieved profiles are most sensitive to the true profile at these pressure levels, e.g., ~500 hPa for TES. The averaging kernels describe the relative contributions to the CO volume mixing ratio (VMR) retrieved at a
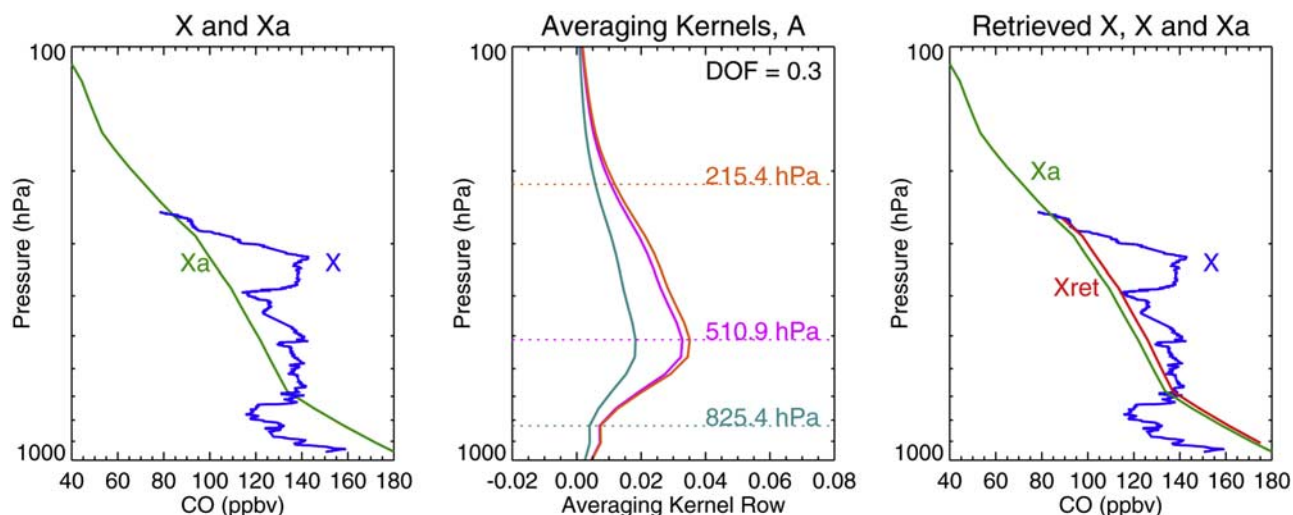
Figure 4. A simulation illustrating the relationship among true, a priori, and the retrieved CO profiles. All three panels are similar to Figure 3. The true CO profile is from the in situ measurement of CO by the DACOM instrument during the Polar Aura Validation Experiment near Portsmouth, 3 February 2005. In this case, the TES retrieval in a close location has DOF of 0.3.

given level of the true and a priori (via $I - A$) CO profiles at all the pressure levels (see equation (1)). For example, in Figure 4, the retrieved CO VMR at 215 or 825 hPa are combinations of the true CO profile with the maximum contribution near 500 hPa and the a priori CO profile at all pressures. The areas under the averaging kernels in Figure 4 are much smaller than those in Figure 3, so the a priori information in the retrieved CO profile is more dominant in the case of Figure 4.

[10] A useful parameter calculated from the information about the measurement and the a priori data is the Degrees of Freedom for signal (DOF), which describes the number of independent pieces of information available in the retrieved vertical profile [*Rodgers*, 2000]. In Figures 3 and 4 for the tropospheric CO profiles, their DOFs are calculated as 1.2 and 0.3, respectively. For the retrieved profiles with DOF less than 1, the a priori profile dominates at most retrieval levels.

[11] Equation (1) without the error term is applied for the cases in Figures 3 and 4. The retrieved CO profiles (x_{ret}) are illustrated together with the true (x) and the a priori profiles (x_a). The profile shapes of the retrieved CO are hardly changed from the a priori profile, and they are not able to follow the complicated shapes of the true CO profiles. The departures of the retrieved CO VMR from the true VMRs at some pressure levels are as large as 40 ppb.

[12] Figures 3 and 4 are presented in order to illustrate the effects of equation (1). Validation of TES retrievals with the aircraft measurements of CO profiles will be presented in a future article. Equation (1) must be applied to the in situ CO measurements to make an appropriate comparison to satellite data [e.g., *Worden et al.*, 2007].

[13] Equation (1) relates the retrieved species profiles provided by the algorithm and the true atmospheric profiles. The choice of the a priori profiles and the associated covariance matrix used in retrieval constraints for TES and MOPITT are described by *Kulawik et al.* [2006a] and *Deeter et al.* [2003], respectively. The averaging kernel

matrix is derived from quantities including the a priori covariance matrix and the instrument and measurement specific parameters (e.g., the sensitivity of the spectral measurements to the profile perturbation at vertical levels, the measurement precision, *etc.*). For the same atmospheric species, different remote sensing instruments and retrieval algorithms would offer different averaging kernels and a priori profiles.

3. TES and MOPITT CO Retrievals

[14] TES is an infrared Fourier Transform Spectrometer [*Beer et al.*, 2001; *Beer*, 2006] and MOPITT is a gas correlation spectrometer [*Drummond and Mand*, 1996]. Both instruments use measurement signals in the CO $(1-0)$ spectral band near 4.7 μm for CO profile retrievals. TES makes nadir measurements along the Aura orbit track with a 1:45 pm ascending equator crossing. The TES nadir footprints of 5×8 km are separated by over 500 km before 21 May 2005 and by under 200 km thereafter. MOPITT makes cross orbit track scans to about ±350 km with a nadir footprint of 22×22 km. Terra satellite has a 9:30 am ascending equator-crossing times, so that the orbits of Aura and Terra are not overlapping on the same day, as illustrated in Figure 2. In this study, we use data version 2 for TES and data version 3 for MOPITT.

[15] Descriptions of TES and MOPITT retrievals of CO profiles are given elsewhere [*Bowman et al.*, 2006; *Clough et al.*, 2006; *Deeter et al.*, 2003]. The two instrument teams use optimal estimation retrieval technique with explicit profile a priori and covariance constraints. TES uses MOZART model data [*Brasseur et al.*, 1998] binned by month and in blocks of 10° by 60° (latitude by longitude) as a priori profiles [*Kulawik et al.*, 2006a]. For the version 3 data, MOPITT chose to use a single CO a priori profile derived from several hundred in situ CO profiles distributed globally [*Deeter et al.*, 2003]. The constraint matrices used for CO profile retrievals are also different for the two
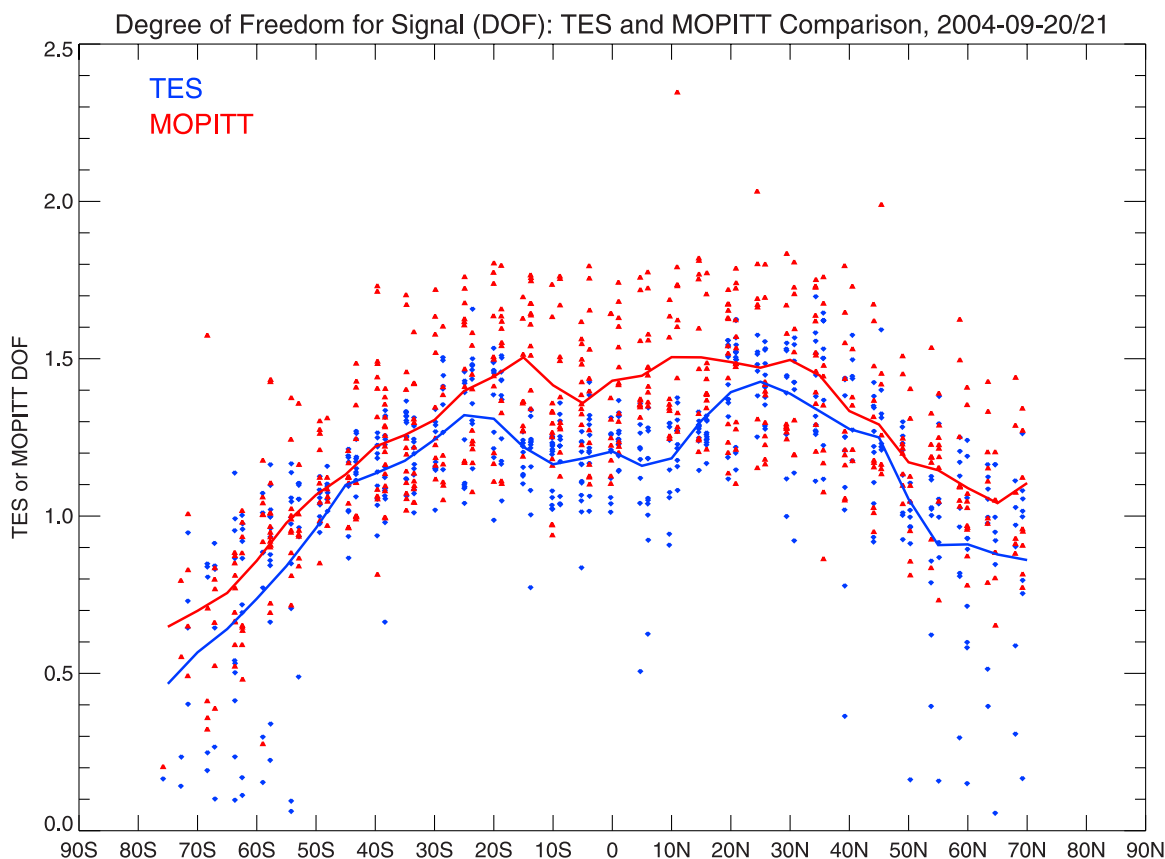
Figure 5. Degrees of Freedom for Signal (DOF) of CO profile retrievals as a function of latitude from TES (blue) and MOPITT (red). MOPITT data are selected for each TES data point at closest location in a TES global survey period of 20–21 September 2004. Latitude averages in a ±5° bin are shown in solid curves for the two instruments.

instruments. TES uses modified Tikhonov constraints [*Kulawik et al.*, 2006a] and MOPITT uses the covariance matrix derived from the ensemble of in situ CO measurements [*Deeter et al.*, 2003]. This is important because in addition to different instrument characteristics, the constraint matrices determine the averaging kernels for the two instruments.

[16] The first step in comparing TES and MOPITT was to choose measurements close in time and location. We selected one TES global survey (∼26 hr) from 20–21 September 2004 and obtained the corresponding MOPITT profiles. Figure 2 shows all the MOPITT measurements in this time period and the TES geolocations. For each TES profile, a MOPITT profile is selected that is closest to the TES location and within 500 km. Even though the variability of CO fields in space and time will affect the comparisons, we did test the use of more restricted location limits (e.g., 200 and 100 km) and determined that this does not alter the conclusions of this study.

[17] The Degrees of Freedom for signal (DOF) for TES and MOPITT are plotted as a function of latitude in Figure 5. The ±5° latitude running averages of the DOFs are represented as solid curves. Both TES and MOPITT have DOFs between 0.5 and 2, except at high latitudes. MOPITT DOFs are slightly higher than those of TES at all latitudes. Near the tropics and under clear sky conditions, the DOFs are greater than one.

[18] The total retrieval errors reported by both instruments are shown in Figure 6 for three pressure levels. Both instruments estimate that the total error is dominated by the smoothing error [*Bowman et al.*, 2006; *Deeter et al.*, 2003], so the results from this comparison indicate that TES has a tighter constraint between vertical levels than does MOPITT at most latitudes. This is also reflected in the DOF comparisons. The error estimates for TES retrievals use the a priori covariance matrices derived from the MOZART model but the constraint matrices in the retrieval processes are the Tikhonov method with first derivatives based on those a priori covariance matrices [*Kulawik et al.*, 2006a]. This difference explains the cases in southern high latitudes where TES total errors are greater than the a priori errors in Figure 6.

4. TES and MOPITT CO Retrieval Comparisons

[19] Here we present comparisons between CO profiles and total columns reported by TES and MOPITT, using data for 20–21 September 2004 as described above. Vertical interpolation is used to match TES and MOPITT pressure levels, reported at about 25 and 7 levels in the troposphere, respectively. We first compare CO VMR from the two instruments directly at the common pressure levels. We then make adjustments of TES or MOPITT profiles by simulating the CO profiles that the two instruments would
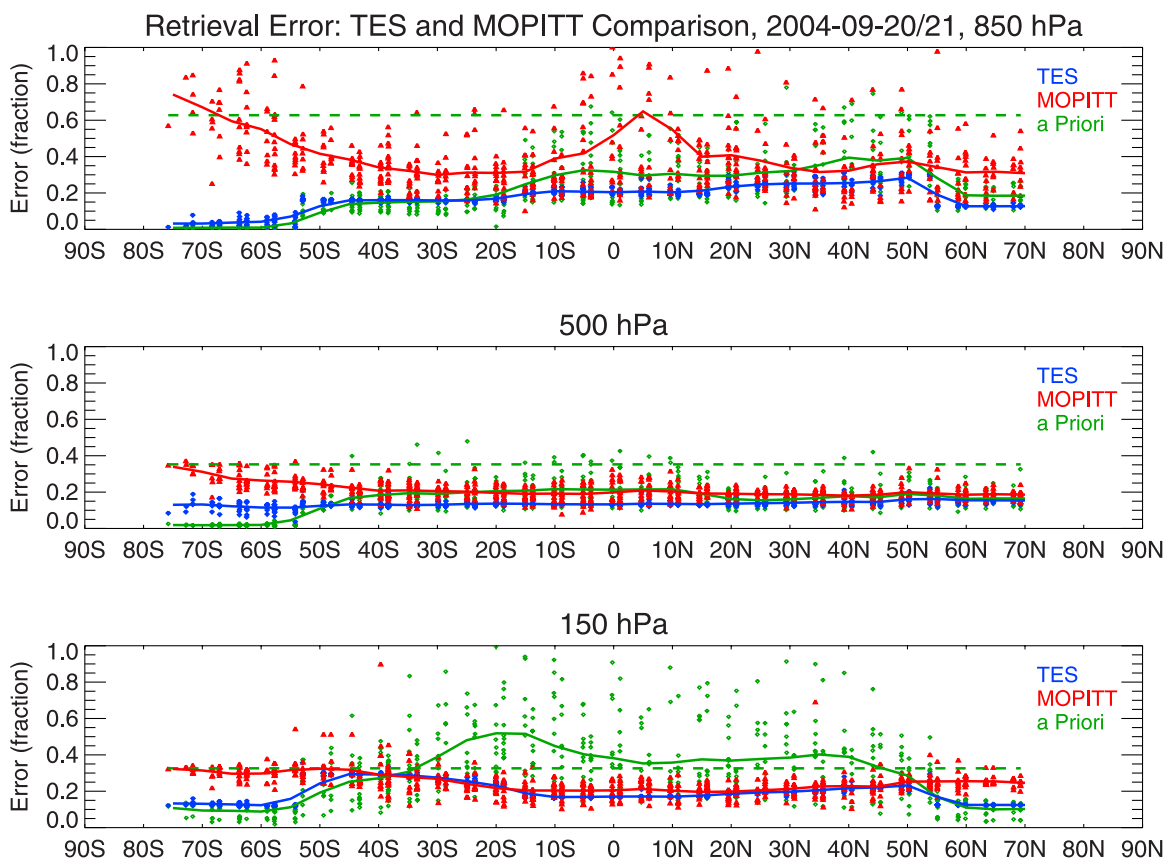
Figure 6. Total CO retrieval errors, as a fraction of the retrieved mixing ratio, reported by TES (blue) and MOPITT (red) and the a priori errors (also as a fraction) (TES = green dots and solid green curve, and MOPITT = dashed green curve) at three pressure levels, 850, 500, and 150 hPa. Solid curves are latitude averages with a bin size of 10° latitude.

retrieve via applying the same a priori and averaging kernels. Total columns calculated from the CO profiles are also compared.

4.1. Direct Comparisons

[20] Figure 7 shows the comparisons of CO VMR at 850, 500 and 150 hPa, and the total column of CO for TES and MOPITT data along with the a priori for each instrument. Running averages as a function of latitude are shown in solid curves. The agreement between TES and MOPITT is best at 500 hPa. Both instruments are most sensitive to CO in the mid troposphere, as shown by the peaks in the TES averaging kernels. MOPITT averaging kernels have similar shapes [Deeter et al., 2004]. The CO retrievals from both instruments should be closer to the true profile at 500 hPa than the retrievals at other levels.

[21] The TES CO retrievals follow the a priori CO at 850 hPa over most of the globe except in regions with enhanced CO due to biomass burning. The MOPITT CO retrievals in the Southern Hemisphere (SH) are larger than that of TES and tend to follow the MOPITT a priori in this region. The dominant role of the a priori profile to the retrievals where both instruments have little information from the measurements is illustrated best by the comparisons in the SH.

[22] The latitudinal dependence of CO VMR at 150 hPa from each instrument follows that of its a priori. The

MOPITT CO is almost uniform as a function of latitude due to the constant a priori, while TES CO follows the latitude pattern defined by the MOZART model.

[23] The total CO column is derived from the profile, so the influence of the a priori and the averaging kernel on the retrieval profile is propagated to the total column. The difference between TES and MOPITT CO columns as a function of latitude is similar to that of 850 hPa, e.g., higher MOPITT CO in the SH.

4.2. TES Retrievals Adjusted to MOPITT A Priori

[24] Direct comparison between TES and MOPITT CO profiles is not appropriate because of the different a priori profiles used in the retrievals. Rodgers and Connor [2003] derived an equation to adjust a retrieval profile for a different a priori so that a more realistic comparison can be made between retrievals that use different a priori. Here we adjust TES CO retrievals (x_{ret}^{TES}) to the MOPITT a priori (x_a^{MOP}) via the following equation

$$x_{adj}^{TES} = x_{ret}^{TES} + \left(A^{TES} - I\right)\left(x_a^{TES} - x_a^{MOP}\right) \qquad (2)$$

where x_a^{TES} is the TES a priori profile and A^{TES} is the TES averaging kernel matrix.

[25] The comparisons between the adjusted TES CO profiles, x_{adj}^{TES}, and the MOPITT CO retrieval profiles, x_{ret}^{MOP}, are shown in Figure 8. Improvement is seen at each level and in the total CO column. At 850 hPa and for the total
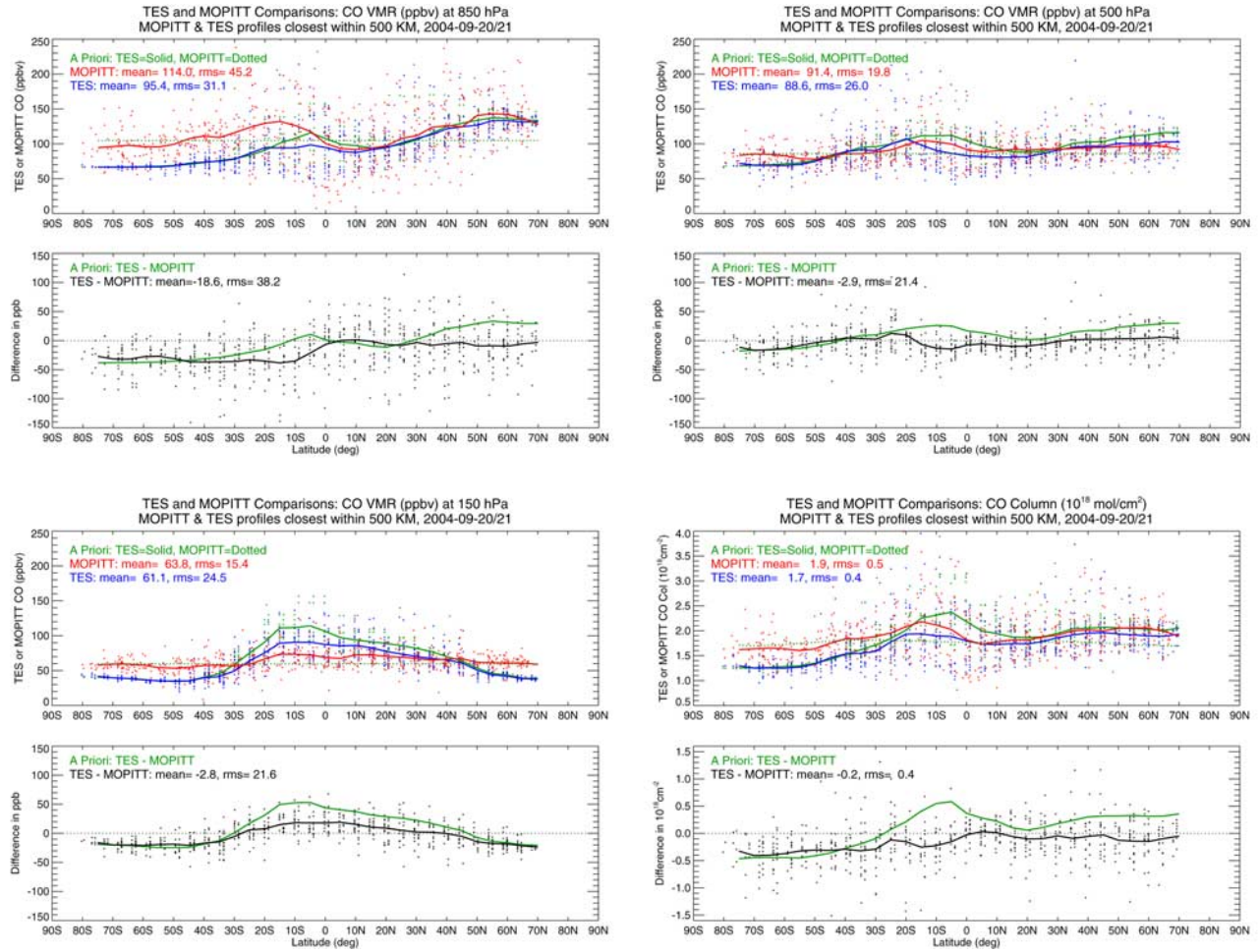
Figure 7. Comparisons of CO Volume Mixing Ratio (VMR) at three pressure levels, 850, 500, and 150 hPa and the total CO column reported by TES and MOPITT. For each pressure level or the total column, there are two panels, the TES and MOPITT data comparison and the difference between TES and MOPITT. In each top panel, TES and MOPITT CO VMR are shown in blue and red, respectively, and the TES and MOPITT a priori are shown in green with TES averages being shown as solid curves and MOPITT single value being shown as a dashed line. In each bottom panel, CO VMRs of TES minus MOPITT are shown in black, and the difference in a priori is shown in green. The global averages (mean) and the root mean squares (rms) of the comparison data are provided.

column, the discrepancies between TES and MOPITT CO in the SH are significantly reduced over the direct comparison. At 150 hPa, TES CO becomes more uniform once it is no longer influenced by the latitudinally dependent a priori, and it agrees much better with the MOPITT CO.

[26] Adjusting MOPITT CO retrievals with TES a priori CO profiles and comparing the MOPITT adjusted profiles with TES retrievals (not shown here) yields the same conclusions. Better agreement is achieved at all levels and for the total CO columns.

4.3. MOPITT Retrievals Smoothed by TES Averaging Kernels

[27] TES and MOPITT have similar but not identical averaging kernels for CO retrievals. The next step in performing proper comparisons is to adjust for the effect of different averaging kernels of one instrument to the other. Unlike adjusting a priori profiles, this adjustment is not reversible [*Rodgers and Connor*, 2003]. Figure 5 indicates

that the MOPITT retrieval algorithm produces slightly higher DOFs for CO profiles than does that of TES, so the TES averaging kernels are applied to MOPITT retrievals to obtain the vertically smoothed MOPITT CO profiles [*Rodgers and Connor*, 2003], x_{smooth}^{MOP},

$$x_{smooth}^{MOP} = A^{TES} x_{ret}^{MOP} + \left(I - A^{TES}\right) x_a^{MOP} \qquad (3)$$

where x_a^{MOP} is the MOPITT a priori profile, x_{ret}^{MOP} is the MOPITT retrieved CO profile, and A^{TES} is the averaging kernel matrix from TES.

[28] The MOPITT CO retrievals smoothed by the TES averaging kernels (x_{smooth}^{MOP}) are compared with the TES CO retrievals adjusted to MOPITT a priori (x_{adj}^{TES}) in Figure 9. The agreement between TES and MOPITT CO profiles is further improved for all levels and for the total column. No systematic differences are found between the adjusted CO profile retrievals from the two instruments.
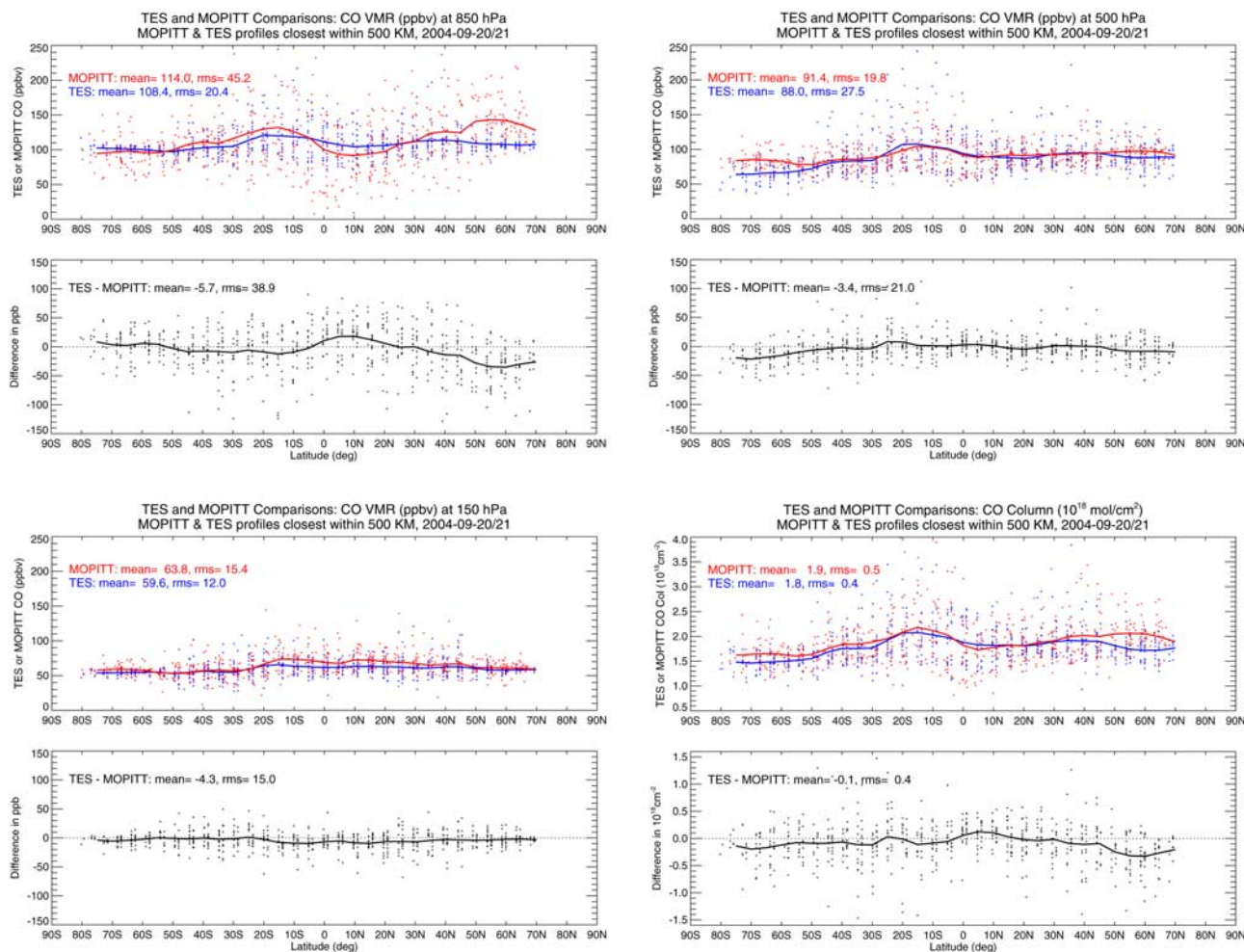
Figure 8. Similar to Figure 7, this figure shows the comparison between TES and MOPITT CO VMR at three pressure levels and the total column. TES CO profiles are adjusted to MOPITT a priori profile via equation (2).

[29] Figures 10 and 11 show two examples of profile comparisons at two representative locations, in northern Brazil and in the Southern Ocean. Figure 10 is a case where the DOFs for TES and MOPITT retrievals are greater than one. The CO retrievals from both instrument teams are different from the a priori but still closely follow the profile shapes of the a priori. After adjusting to the MOPITT a priori, the TES CO profile shape changes and the CO VMR near the surface increases from 120 ppb to nearly 145 ppb. After adjusting to the TES averaging kernel, the MOPITT CO profile shape also changes and the CO VMR near the surface decreases from 170 ppb to 140 ppb. In this comparison, the TES CO profile adjusted to the MOPITT a priori and the MOPITT CO profile smoothed by the TES averaging kernel agree well.

[30] Figure 11 represents a case where the two instruments have DOFs less than 0.5. The TES CO retrieval is nearly identical to its a priori and changes to follow that of the MOPITT a priori in the lower and upper troposphere after adjusting to the MOPITT a priori. After the MOPITT CO profile is smoothed by the TES averaging kernel, it became closer to its a priori because of less information from the measurement.

[31] Table 1 presents a summary of the comparisons. For each of the 3 pressure levels and the total column, we give the global average of the percent difference between each pair of TES and MOPITT CO (%diff) and the percent root mean square (%rms) of the differences globally with respect to the global CO averages of TES and MOPITT. The %diff represents differences between the CO values of the two instruments averaged globally. This could be misleading because of latitudinal dependencies of the comparison, e.g., at 150 hPa when the CO values are compared directly. The %rms however, indicates the spread of the disagreements between CO values of the two instruments. At all pressure levels and the total column, the %rms is reduced by each step in the comparisons. The %rms is not changed much in the middle troposphere (500 hPa) where both instrument have maximum sensitivity. The %rms near the boundary and the upper troposphere are reduced the most in going from the direct comparisons to the comparisons with the same a priori and smoothing of MOPITT by the TES averaging kernels. This is expected since the CO values in these regions are more influenced by the a priori profiles.

[32] Even with proper treatment of the comparisons, several factors remain that contribute to the globally aver-
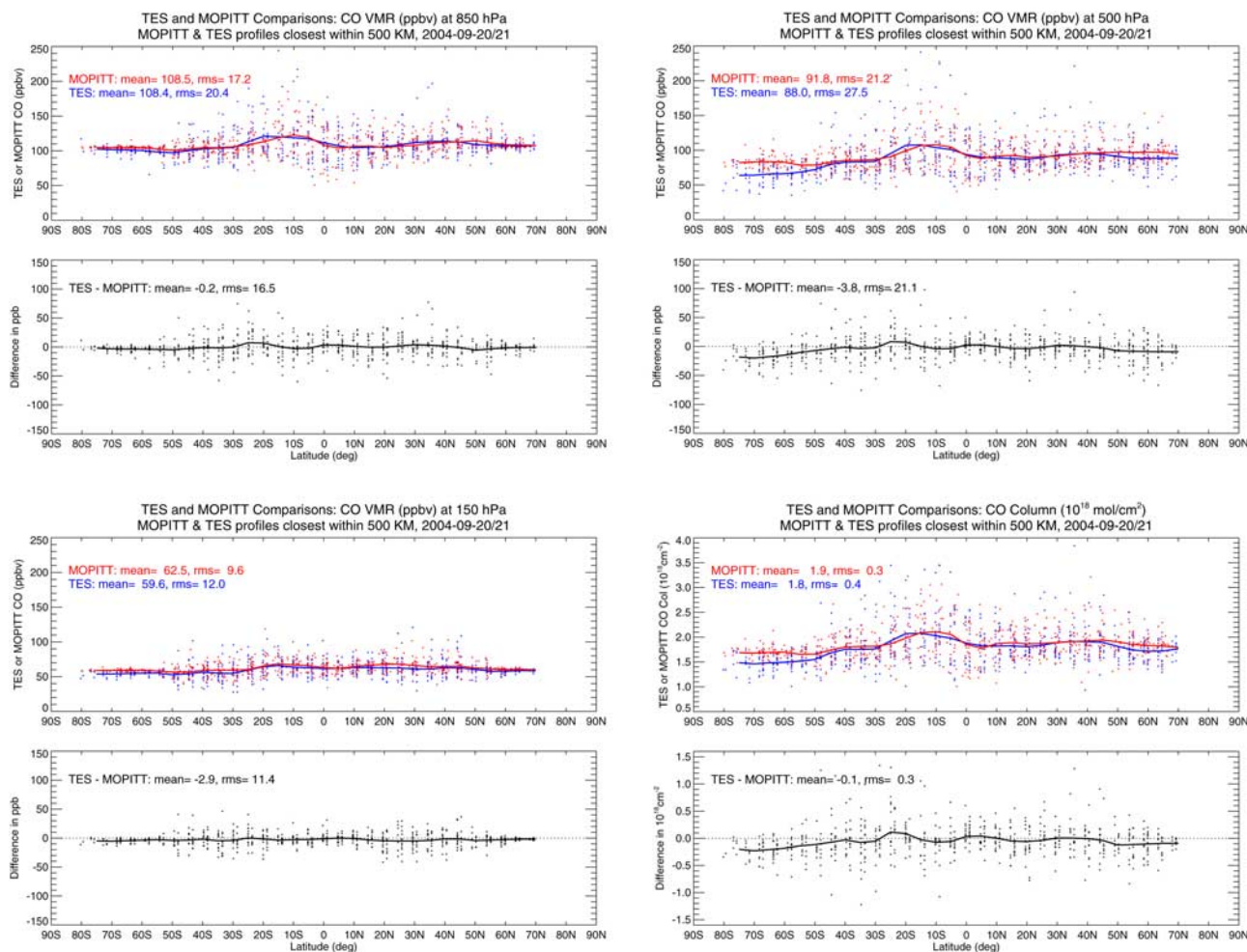
Figure 9. Similar to Figures 7 and 8, this figure shows the comparison between TES and MOPITT CO VMR at three pressure levels and the total column. TES CO profiles are adjusted to MOPITT a priori profile via equation (2). MOPITT CO profiles are adjusted by applying TES averaging kernels via equation (3).

aged differences between TES and MOPITT. First, the spatial and temporal coincidences are not exact, which is important when there are large gradients in CO especially near source regions and dynamically active regions. The vertical interpolation of the MOPITT profile (7 levels for retrieved profiles and 35 levels for the a priori profile) to the finer TES levels (~25 levels in the troposphere) also have minor effects on the comparisons. A more rigorous study of the effects of vertical mapping is presented by *Calisesi et al.* [2005] and it requires many more parameters from the two algorithms that are not routinely available. Another factor is that the TES profiles are retrieved for values of effective cloud optical depth in the range zero to five [*Kulawik et al.*, 2006b]. The parts of the TES CO profile within or below the clouds are very similar to the a priori profile. However, the majority of the MOPITT CO profiles are derived from clear or nearly clear sky conditions.

[33] The comparison error can be calculated [*Rodgers and Connor*, 2003], but it could not be done in this study because of lack of parameters given with the MOPITT standard products (measurement and systematic errors). The comparison error should be slightly larger than the

larger retrieval precision of the two instruments [*Rodgers and Connor*, 2003]. The total CO errors for both TES and MOPITT retrieval products are dominated by the smoothing errors and the two instruments report typical CO retrieval precision of ~10% in the middle troposphere [*Pan et al.*, 1998; *Bowman et al.*, 2006].

5. Discussion and Conclusions

[34] This paper illustrates how the retrieved CO profiles and the calculated total columns reported by the TES and MOPITT teams depend on the a priori data chosen for the retrievals and the measurement characteristics. Two key parameters are explicitly used to illustrate the effect, the a priori profiles and the averaging kernels describing the vertical smoothing that occurs in the retrieval processes. We illustrated the roles that these two parameters play in the relationship between the true and the retrieved CO profiles using comparisons with aircraft data.

[35] The TES and MOPITT teams chose two different approaches in selecting a priori profiles; spatially and temporally variable profiles derived from the MOZART
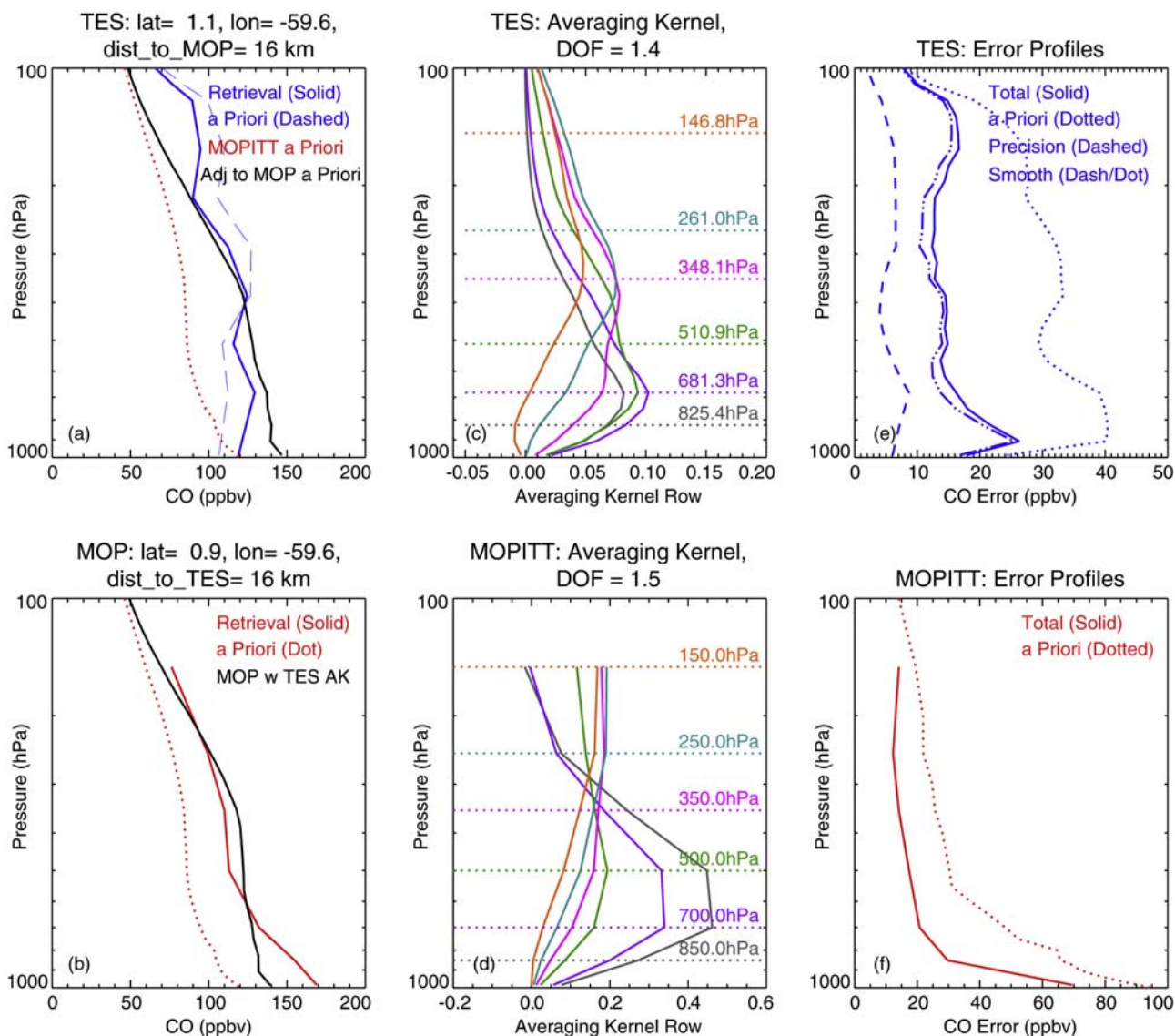
Figure 10. Comparisons of TES and MOPITT retrieved CO profiles in north Brazil, 20 September 2004. (a) TES retrieved CO profile (solid blue curve) and the associated a priori profile (dashed blue curve), the MOPITT a priori (red dotted curve), and the TES retrieval adjusted to the MOPITT a priori (solid black curve). (b) MOPITT retrieved CO profile (solid red curve) and the associated a priori (red dotted curve), and the MOPITT retrieval with TES averaging kernel applied (solid black curve). (c and d) The averaging kernel at six pressure levels from the two instruments. The Degree of Freedom for signal (DOF) is 1.4 and 1.5 for TES and MOPITT. (e and f) Retrieval error breakdown for the two instruments.

model for TES, and a uniform profile derived from in situ data that is constant in time, for MOPITT. We showed that if TES and MOPITT are compared without taking into account the different a priori used in each retrieval, the CO profiles disagree with each other. After we adjusted the TES CO retrievals to the MOPITT a priori profiles or vice versa, better agreements was achieved. After the TES averaging kernels are applied to the MOPITT retrievals to further smooth the MOPITT profiles vertically, the agreement improved further, showing no systematic differences. The agreement shows that there is consistency between MOPITT and TES in respect to their spectral and radiometric calibrations and the spectral data used in forward models. The much improved agreement between TES and MOPITT CO values for the lower and upper troposphere (e.g., 850 hPa and 150 hPa) and for the total column indicates that the influence of the a priori data is the strongest for these levels.

[36] Profiles of atmospheric species derived from satellite remote sensing instruments, such as tropospheric CO profiles from TES and MOPITT, provide much needed data for research in tropospheric chemistry and transport. Appropriate consideration of the profile retrieval process and utilization of additional data products describing the retrievals, e.g., averaging kernel, a priori data and error breakdowns, are essential in any quantitative analysis involving such satellite data.
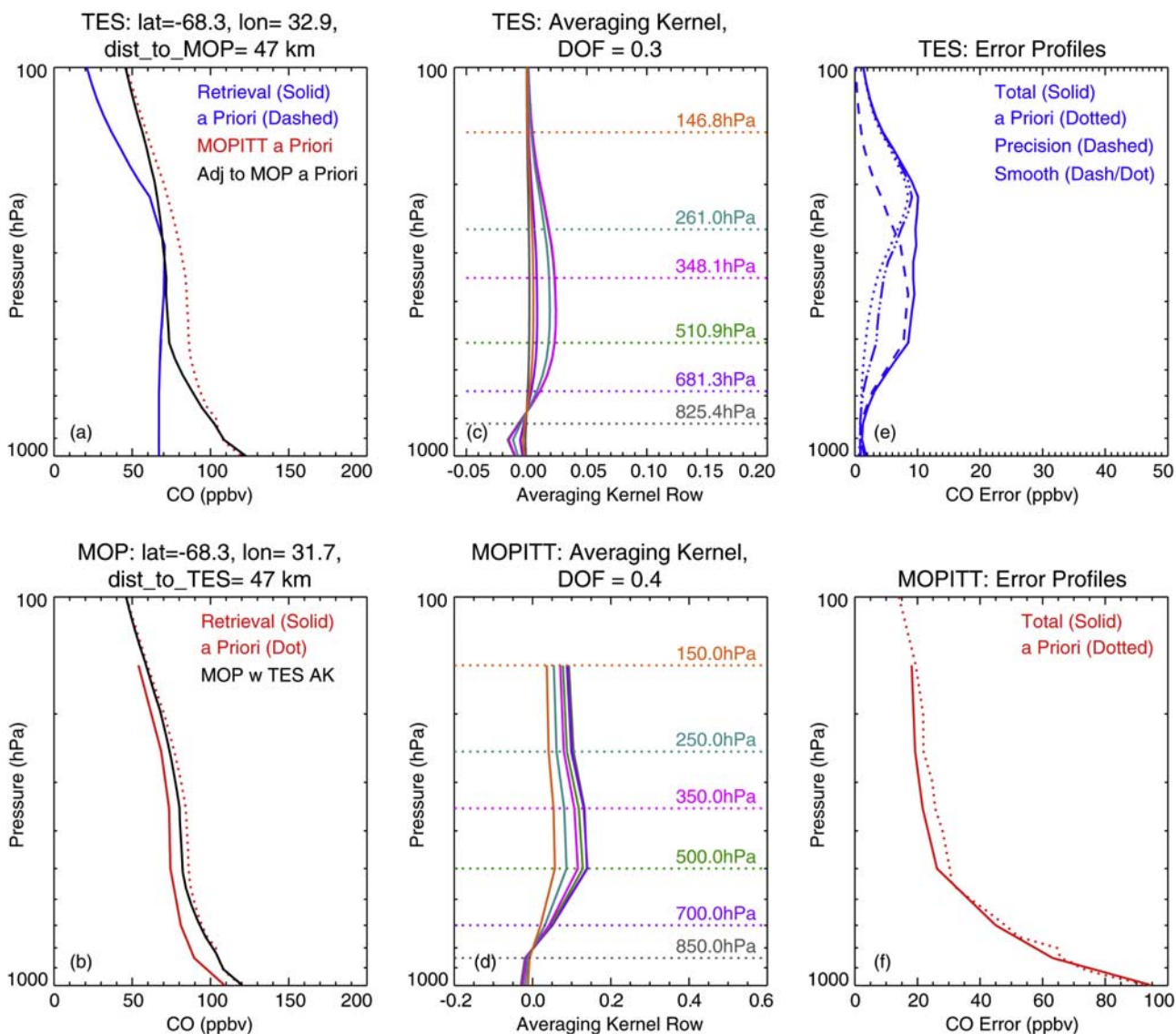
Figure 11. Similar to Figure 10, comparisons of TES and MOPITT retrieved CO profiles over ocean in Southern Hemisphere, 20 September 2004. The Degree of Freedom for signal (DOF) for this case is 0.3 and 0.4 for TES and MOPITT, respectively.

Table 1. Comparisons of Global Averages of TES and MOPITT Reported CO Volume Mixing Ratios at Three Pressure Levels and Total Column for Data Taken 20–21 September 2004[a]

	850 hPa		500 hPa		150 hPa		Total Column	
	Percent Difference	Percent rms	Percent Difference	Percent rms	Percent Difference	Percent rms	Percent Difference	Percent rms
Direct comparison of TES and MOPITT CO	−18%	36%	−3%	24%	−4.5%	35%	−11%	22%
TES CO adjusted to MOPITT a priori compared to MOPITT CO	−5%	35%	−3.8%	23%	−7%	24%	−5.4%	22%
TES CO adjusted to MOPITT a priori compared to MOPITT CO adjusted to TES averaging kernel	−0.2%	15%	−4%	23%	−4.8%	18.7%	−4.4%	16%

[a]Percent difference is the global average of the differences between the matched Tropospheric Emission Spectrometer (TES) and Measurements of Pollution in the Troposphere (MOPITT) points (TES minus MOPITT) divided by the average of the global averages of TES and MOPITT CO VMRs. Percent rms is the root mean square (rms) of the differences between the matched TES and MOPITT points (TES minus MOPITT) divided by the average of the global averages of TES and MOPITT CO VMRs.

References

Beer, R. (2006), TES on the Aura mission: Scientific objectives, measurements, and analysis overview, *IEEE Trans. Geosci. Remote Sens.*, *44*, 1102–1105.

Beer, R., T. A. Glavich, and D. M. Rider (2001), Tropospheric Emission Spectrometer for the Earth Observing System Aura satellite, *Appl. Opt.*, *40*, 2356–2367.

Bowman, K. W., et al. (2006), Tropospheric Emission Spectrometer: Retrieval method and error analysis, *IEEE Trans. Geosci. Remote Sens.*, *44*, 1297–1306.

Brasseur, G. P., D. A. Hauglustaine, S. Walters, P. J. Rasch, J.-F. Muller, C. Granier, and X. X. Tie (1998), MOZART: A global chemical transport model for ozone and related chemical tracers: Part 1. Model description, *J. Geophys. Res.*, *103*, 28,256–28,289.

Calisesi, Y., V. T. Soebijanta, and R. van Oss (2005), Regridding of remote soundings: Formulation and application to ozone profile comparison, *J. Geophys. Res.*, *110*, D23306, doi:10.1029/2005JD006122.

Clerbaux, C., J. Gille, and D. Edwards (2004), New directions: Infrared measurements of atmospheric pollution from space, *Atmos. Environ.*, *38*, 4599–4601.

Clough, S. A., et al. (2006), Forward model and Jacobians for Tropospheric Emission Spectrometer retrievals, *IEEE Trans. Geosci. Remote Sens.*, *44*, 1308–1323.

Deeter, M. N., et al. (2003), Operational carbon monoxide retrieval algorithm and selected results from the MOPITT instrument, *J. Geophys. Res.*, *108*(D14), 4399, doi:10.1029/2002JD003186.

Deeter, M. N., L. K. Emmons, D. P. Edwards, J. C. Gille, and J. R. Drummond (2004), Vertical resolution and information content of CO profiles retrieved by MOPITT, *Geophys. Res. Lett.*, *31*, L15112, doi:10.1029/2004GL020235.

Drummond, J. R., and G. S. Mand (1996), The Measurement of Pollution in the Troposphere (MOPITT) instrument: Overall performance and calibration requirements, *J. Atmos. Oceanic Technol.*, *13*, 314–320.

Edwards, D. P., et al. (2004), Observations of carbon monoxide and aerosols from the Terra satellite: Northern Hemisphere variability, *J. Geophys. Res.*, *109*, D24202, doi:10.1029/2004JD004727.

Emmons, L. K., et al. (2004), Validation of Measurements of Pollution in the Troposphere (MOPITT) CO retrievals with aircraft in situ profiles, *J. Geophys. Res.*, *109*, D03309, doi:10.1029/2003JD004101, 2004.

Kulawik, S. S., G. Osterman, D. B. A. Jones, and K. W. Bowman (2006a), Calculation of altitude-dependent Tikhonov constraints for TES nadir retrievals, *IEEE Trans. Geosci. Remote Sens.*, *44*, 1334–1342.

Kulawik, S. S., J. Worden, A. Eldering, K. Bowman, M. Gunson, G. B. Osterman, L. Zhang, S. A. Clough, M. W. Shephard, and R. Beer (2006b), Implementation of cloud retrievals for Tropospheric Emission Spectrometer (TES) atmospheric retrievals: part 1. Description and characterization of errors on trace gas retrievals, *J. Geophys. Res.*, *111*, D24204, doi:10.1029/2005JD006733.

Osterman, G., et al. (2005), Tropospheric emission spectrometer (TES) validation report, *JPL D33192, version 1.0*, Jet Propul. Lab., Pasadena, Calif. (Available at http://tes.jpl.nasa.gov/docsLinks/documents.cfm)

Pan, L., J. C. Gille, D. P. Edwards, P. L. Bailey, and C. D. Rodgers (1998), Retrieval of tropospheric carbon monoxide for the MOPITT experiment, *J. Geophys. Res.*, *103*, 32,277–32,290.

Rinsland, C. P., et al. (2006), Nadir measurements of carbon monoxide distributions by the Tropospheric Emission Spectrometer instrument onboard the Aura Spacecraft: Overview of analysis approach and examples of initial results, *Geophys. Res. Lett.*, *33*, L22806, doi:10.1029/2006GL027000.

Rodgers, C. D. (2000), *Inverse Methods for Atmospheric Sounding: Theory and Practice*, World Sci., Hackensack, N. J.

Rodgers, C. D., and B. J. Connor (2003), Intercomparisons of remote sounding instruments, *J. Geophys. Res.*, *108*(D3), 4116, doi:10.1029/2002JD002299.

Sachse, G. W., G. F. Hill, L. O. Wade, and M. G. Perry (1987), Fast-response, high-precision carbon monoxide sensor using a tunable diode laser absorption technique, *J. Geophys. Res.*, *92*, 2071–2081.

Worden, H. M., et al. (2007), Comparisons of Tropospheric Emission Spectrometer (TES) ozone profiles to ozonesondes: Methods and initial results, *J. Geophys. Res.*, *112*, D03309, doi:10.1029/2006JD007258.

_____

A. Eldering, M. Gunson, S. Kulawik, M. Luo, and H. Worden, Jet Propulsion Laboratory, California Institute of Technology, 4800 Oak Grove Drive, Pasadena, CA 91109, USA. (mluo@jpl.nasa.gov)

A. Goldman, Department of Physics, University of Denver, Denver, CO 80208, USA.

M. Lampel, Raytheon Information Solutions, 299 North Euclid Avenue, Suite 500, Pasadena, CA 91101, USA.

J. A. Logan, Division of Engineering and Applied Sciences, Harvard University, Cambridge, MA 02138, USA.

C. P. Rinsland, NASA Langley Research Center, Mail Stop 401A, Hampton, VA 23681-2199, USA.

C. D. Rodgers, Clarendon Laboratory, Oxford University, Oxford OX1 3PU, UK.

M. W. Shephard, Atmospheric and Environmental Research Incorporated (AER), 131 Hartwell Avenue, Lexington, MA 02421, USA.